Nanoscale Advances

ROYAL SOCIETY OF CHEMISTRY

PAPER

View Article Online
View Journal | View Issue

Cite this: *Nanoscale Adv.*, 2023, **5**, 4863

Entropy generation in bioconvection hydromagnetic flow with gyrotactic motile microorganisms

Sohail A. Khan, *[a] T. Hayat[a] and A. Alsaedi [b]

Here, the magnetohydrodynamic bioconvective flow of a non-Newtonian nanomaterial over a stretched sheet is scrutinized. The characteristics of convective conditions are analyzed. Irreversibility analysis in the presence of gyrotactic micro-organisms is discussed. Energy expression is assisted with thermal radiation, heat generation and ohmic heating. Buongiorno's model is employed to discuss the characteristics of the nanoliquid through thermophoresis and random diffusions. Nonlinear expressions of the given model are transformed through adequate transformations. The obtained expressions have been computed by the Newton built in-shooting technique. Results of influential variables for velocity, concentration, microorganism field, temperature and entropy rate are graphically studied. Clearly, velocity reduction is witnessed for the bioconvection Rayleigh number and magnetic variable. A higher heat generation variable leads to augmentation of temperature. An increase in the magnetic variable results in entropy and temperature enhancement. A higher Peclet number results in microorganism field reduction. Temperature distribution rises for radiation and the thermal Biot number. A higher solutal Biot number intensifies the concentration. The entropy rate for radiation and diffusion variables is enhanced.

Received 18th May 2023
Accepted 7th August 2023

DOI: 10.1039/d3na00338h

rsc.li/nanoscale-advances

1 Introduction

Recently, nanotechnology has gained much consideration amongst researchers and investigators. It is due to its involvement in chemical processes, microelectronics, engineering, hybrid powered engines and biological processes. Nanomaterials are basically homogeneous colloidal suspensions of nano-size (1–10 nm) particles in an ordinary liquid which enhances the thermal conductivity of conventional liquids.[1,2] Nanofluids have specific characteristics that make them more applicable materials. Nanomaterials have innovative characteristics about heat transfer enhancement. Buongiorno[3] gave a theoretical model for heat transport rate enhancement of conventional liquids. He highlighted that only random and thermophoresis diffusions are main mechanisms for thermal transportation enhancement. Nanomaterials are very significant in improving the thermal productivity of hybrid power engines, electronic devices, nuclear system chillers, domestic refrigerators and many others. Shahzad *et al.*[4] analyzed the bioconvection convectively heated micropolar nanomaterial flow between two rotating disks. The mixed convective magnetohydrodynamic flow of a viscoelastic nanomaterial with heat generation was discussed by Waqas *et al.*[5] Anjum *et al.*[6] explored activation energy in the bioconvective MHD flow of a modified Eyring–Powell nanomaterial. Mabood *et al.*[7] reported chemically reactive micropolar nanoliquid flow considering thermal radiation. Numerical analysis of hydromagnetic unsteady nanomaterial flow towards an irregular stretched sheet was reported by Kalpana *et al.*[8] Thermal analysis for the hydromagnetic flow of a nanomaterial subject to entropy was addressed in Riaz *et al.*[9] Further investigations about nanomaterial flow are highlighted through ref. 10–17.

In recent years the bioconvection phenomenon in nanomaterials along motile microorganisms has attracted much attention from researchers. It is because of its significance in tremendous engineering, pharmaceutical and biological processes in fields such as biofuel, biomedicine, fertilizer, biotechnology, bio-microsystem and enzyme biosensor. Bioconvection occurs due to up swimming of microorganisms. Commonly the density of microorganisms is heavier than the base fluid and therefore it raises unsteady upper surface density stratification.[18,19] Bio convection is extensively used in environmental science, conversion in engineering, bio-microsystems, biological processes with microbial-upgraded oil recovery systems, enzyme biosensors, mass transport and bioengineering in biotechnology and the ecosystem. Prime utilization of this mechanism is to enhance the capacity of appropriate fraternization and mass transfer. Bio convection refers to macroscopic movement of liquid induced by a density gradient organized by an alternating floating system based on motile microbes. Thermal radiation impact in a bioconvective

[a]*Department of Mathematics, Quaid-I-Azam University 45320, Islamabad 44000, Pakistan. E-mail: sohailahmadkhan93@gmail.com*

[b]*Nonlinear Analysis and Applied Mathematics (NAAM) Research Group, Faculty of Science, King Abdulaziz University, P. O. Box 80207, Jeddah 21589, Saudi Arabia*

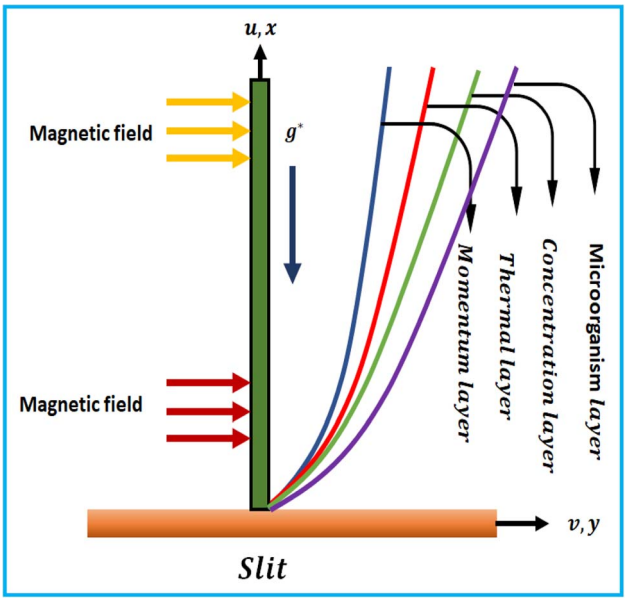

Fig. 1 Flow configuration.

ferromagnetic Williamson material subject to dissipation was studied by Kada *et al.*[20] Majeed *et al.*[21] highlighted the features of gyrotactic microorganisms in magnetized time-dependent nanoliquid flow. Waqas *et al.*[22] scrutinized thermo and solutal stratification impacts in Casson nanomaterial flow with convective boundary conditions. Azam *et al.*[23] examined activation in the bioconvection flow of a cross nanoliquid subject to gyrotactic microorganisms. Some interesting explorations of bioconvective flow can be seen in Ref. 24–32.

Motivation of current analysis is to address the bioconvective flow of the Reiner–Rivlin nanoliquid. Gyrotactic microorganisms in the presence of convective conditions are discussed. The characteristics of thermophoresis and random diffusions are analyzed. Energy expression consists of radiation, heat generation and ohmic heating. Irreversibility analysis along with chemical reaction is analyzed. The Newton built in-shooting technique (ND-solve) is employed to develop numerical solutions of the considered model. Graphical analysis illustrating the influence of liquid flow, concentration, microorganism field, temperature and entropy rate is organized. Main results are listed in conclusion.

2 Formulation

Here the flow of the bioconvection Reiner–Rivlin nanomaterial past a stretched boundary is examined. Convective conditions along with chemical reaction are analyzed. Thermophoresis, random diffusion and involvement of motile microorganisms are considered. Influences of radiation, magnetic field and heat generation are considered. Physical impact for the entropy rate is explored. A uniform magnetic field of strength (B_0) is applied. The surface is stretched with velocity ($u_w = ax$) subject to rate constant ($a > 0$). Fig. 1 consists of flow configuration.[33]

Under the above assumptions, the related equations are:[34–38]

$$\frac{\partial u}{\partial x}+\frac{\partial v}{\partial y}=0, \tag{1}$$

$$\left.\begin{aligned} u\frac{\partial u}{\partial x}+v\frac{\partial u}{\partial y}&=\nu_f\frac{\partial^2 u}{\partial y^2}+2\frac{\mu_c}{\rho_f}\left(\frac{\partial u}{\partial y}\frac{\partial^2 u}{\partial x\partial y}+\frac{\partial u}{\partial x}\frac{\partial^2 u}{\partial y^2}\right)-\frac{\sigma_f {B_0}^2}{\rho_f}u\\ &+\frac{1}{\rho_f}\left(\rho_f(1-C_\infty)g^*\beta^*(T-T_\infty)-g^*(\rho_p-\rho_f)(C-C_\infty)-g^*\gamma^*(\rho_m-\rho_f)(N-N_\infty)\right)\end{aligned}\right\}, \tag{2}$$

$$\left.\begin{aligned} u\frac{\partial T}{\partial x}+v\frac{\partial T}{\partial y}&=\frac{k_f}{(\rho c_p)_f}\frac{\partial^2 T}{\partial y^2}+\frac{16\sigma^* {T_\infty}^3}{3k^*(\rho c_p)_f}\frac{\partial^2 T}{\partial y^2}+\frac{\sigma_f {B_0}^2}{(\rho c_p)_f}u^2+\tau\left(\frac{D_B}{\Delta C}\frac{\partial T}{\partial y}\frac{\partial C}{\partial y}+\frac{D_T}{T_\infty}\left(\frac{\partial T}{\partial y}\right)^2\right)\\ &+\frac{Q_0}{(\rho c_p)_f}(T-T_\infty)\end{aligned}\right\}, \tag{3}$$

$$u\frac{\partial C}{\partial x}+v\frac{\partial C}{\partial y}=D_B\frac{\partial^2 C}{\partial y^2}+\frac{\Delta C D_T}{T_\infty}\frac{\partial^2 T}{\partial y^2}-k_r(C-C_\infty), \tag{4}$$

$$u\frac{\partial N}{\partial x}+v\frac{\partial N}{\partial y}+\frac{bW_c}{(C_w-C_\infty)}\left(\frac{\partial}{\partial y}\left(N\frac{\partial C}{\partial y}\right)\right)=D_m\frac{\partial^2 N}{\partial y^2}, \tag{5}$$

with the boundary condition:[36–38]

$$\left.\begin{aligned} &u=u_w(x)=ax,\quad v=0,\quad -k_f\frac{\partial T}{\partial y}=h_f(T_w-T),\\ &-D_B\frac{\partial C}{\partial y}=h_w(C_w-C),\quad -D_m\frac{\partial N}{\partial y}=h_n(N_w-N)\ \text{at}\ y=0\\ &u\to 0,\quad T\to T_\infty, C\to C_\infty,\quad N\to N_\infty\ \text{as}\ y\to\infty\end{aligned}\right\}. \tag{6}$$

In the above expressions (u,v) denote the velocity components, ν_f the kinematic viscosity, μ_c the cross viscosity, g^* the gravity, (x,y) characterize Cartesian coordinates, β^* the thermal expansion coefficient, ρ_p the particle density, ρ_m the microorganism density, γ^* the average volume of microorganisms, h_f the heat transfer rate, B_0 the magnetic field strength, μ_f the dynamic viscosity, ρ_f the liquid density, b the chemotaxis constant, σ_f the electrical conductivity, h_w the mass transfer rate, T the temperature, D_B the Brownian diffusion coefficient, W_c the cell swimming speed, $Q_0 > 0$ the heat generation coefficient, T_w the wall temperature, τ the ratio of heat capacitance, $\alpha_f = \left(\frac{k_f}{(\rho c_p)_f}\right)$ the thermal diffusivity, $(c_p)_f$ the specific heat, T_∞ the ambient temperature, σ^* the Stefan–Boltzmann constant, D_T the thermophoresis coefficient, k_f the thermal conductivity, h_n the microorganism transfer rate, k^* the mean absorption coefficient, C the concentration, ΔC the concentration difference, C_w the wall concentration, k_r the reaction rate, C_∞ the ambient concentration, N the motile microorganisms, N_w the wall motile microorganisms, D_m the microorganism diffusion coefficient and N_∞ the wall motile microorganisms.

Letting l as the reference length and transformations:[38] one has

$$\left.\begin{aligned} u = ax\frac{\partial f(\xi,\eta)}{\partial \eta},\ \ v = -\sqrt{a\nu_f}\left(f(\xi,\eta) + \xi\frac{\partial f(\xi,\ \eta)}{\partial \xi}\right),\ \ \eta = \sqrt{\frac{a}{\nu_f}}y \\ \theta(\xi,\eta) = \frac{T-T_\infty}{T_w - T_\infty},\ \ \phi(\xi,\ \eta) = \frac{C-C_\infty}{C_w - C_\infty},\ \ \chi(\xi,\eta) = \frac{N-N_\infty}{N_w - N_\infty},\ \ \xi = \frac{x}{l} \end{aligned}\right\}, \tag{7}$$

$$\left.\begin{aligned} \frac{\partial^3 f}{\partial \eta^3} + f\frac{\partial^2 f}{\partial \eta^2} + \xi\frac{\partial f}{\partial \xi}\frac{\partial^2 f}{\partial \eta^2} - \left(\frac{\partial f}{\partial \eta}\right)^2 - \xi\frac{\partial^2 f}{\partial \xi \partial \eta}\frac{\partial f}{\partial \eta} + 2K\left(\begin{aligned} &\left(\frac{\partial^2 f}{\partial \eta^2}\right)^2 + \xi\frac{\partial^2 f}{\partial \eta^2}\frac{\partial^3 f}{\partial \xi \partial \eta^2} \\ &+\frac{\partial f}{\partial \eta}\frac{\partial^3 f}{\partial \eta^3} + \xi\frac{\partial^2 f}{\partial \xi \partial \eta}\frac{\partial^3 f}{\partial \eta^3} \end{aligned}\right) \\ -M\frac{\partial f}{\partial \eta} + \frac{\lambda}{\xi}(\theta - \beta_1^*\phi - \beta_2^*\chi) = 0 \end{aligned}\right\} \tag{8}$$

$$\left.\begin{aligned} (1+\mathrm{Rd})\frac{\partial^2 \theta}{\partial \eta^2} + \mathrm{Pr}\xi\frac{\partial f}{\partial \eta}\frac{\partial \theta}{\partial \eta} + \mathrm{Pr}f\frac{\partial \theta}{\partial \eta} - \mathrm{Pr}\xi\frac{\partial f}{\partial \eta}\frac{\partial \theta}{\partial \xi} + \mathrm{Pr}Q\theta \\ +\mathrm{PrNb}\frac{\partial \theta}{\partial \eta}\frac{\partial \phi}{\partial \eta} + \mathrm{PrNt}\left(\frac{\partial \theta}{\partial \eta}\right)^2 + MEc\mathrm{Pr}\xi^2\left(\frac{\partial f}{\partial \eta}\right)^2 = 0 \end{aligned}\right\}, \tag{9}$$

$$\left.\frac{\partial^2 \phi}{\partial \eta^2} + \mathrm{Sc}f\frac{\partial \phi}{\partial \eta} - \mathrm{Sc}\xi\frac{\partial f}{\partial \eta}\frac{\partial \phi}{\partial \xi} + \mathrm{Sc}\xi\frac{\partial f}{\partial \xi}\frac{\partial \phi}{\partial \eta} + \frac{Nt}{Nb}\frac{\partial^2 \theta}{\partial \eta^2} - \mathrm{Sc}\gamma\phi = 0\right\}, \tag{10}$$

$$\left.\begin{aligned} \frac{\partial^2 \chi}{\partial \eta^2} + \mathrm{Lb}f\frac{\partial \chi}{\partial \eta} - \mathrm{Lb}\xi\frac{\partial f}{\partial \eta}\frac{\partial \chi}{\partial \xi} + \mathrm{Lb}\xi\frac{\partial f}{\partial \xi}\frac{\partial \chi}{\partial \eta} \\ -\mathrm{Pe}\left(\Omega\frac{\partial^2 \phi}{\partial \eta^2} + \frac{\partial \chi}{\partial \eta}\frac{\partial \phi}{\partial \eta} + \chi\frac{\partial^2 \phi}{\partial \eta^2}\right) = 0 \end{aligned}\right\}, \tag{11}$$

$$\left.\begin{aligned} \frac{\partial f(\xi,\ 0)}{\partial \eta} = 1,\ \ f(\xi,\ 0) = -\xi\frac{\partial f(\xi,\ 0)}{\partial \xi}, \frac{\partial \theta}{\partial \eta}(\xi,\ 0) = -\beta_1(1-\theta(\xi,\ 0)) \\ \frac{\partial \varphi}{\partial \eta}(\xi,\ 0) = -\beta_2(1-\phi(\xi,\ 0)),\ \frac{\partial \chi}{\partial \eta}(\xi,\ 0) = -\beta_3(1-\chi(\xi,\ 0)) \\ \frac{\partial f}{\partial \eta}(\xi,\ \infty) = 0,\ \theta(\xi,\infty) = 0,\ \phi(\xi,\infty) = 0,\ \chi(\xi,\infty) = 0 \end{aligned}\right\}. \tag{12}$$

In the above equations $M\left(=\frac{\sigma_f {B_0}^2}{a\rho_f}\right)$ represents the magnetic variable, $\beta_1^*\left(=\frac{(\rho_p-\rho_f)(C_w-C_\infty)}{\rho_f(1-C_\infty)(T_w-T_\infty)\beta^*}\right)$ the buoyancy ratio variable, $\lambda\left(=\frac{g\beta^*(1-C_\infty)(T_w-T_\infty)}{a^2 l}\right)$ the mixed convection variable, $K\left(=\frac{\mu_c a}{\nu_f \rho_f}\right)$ the material variable, $\beta_2^*\left(=\frac{(\rho_m-\rho_f)(N_w-N_\infty)\gamma^*}{\rho_f(1-C_\infty)(T_w-T_\infty)\beta^*}\right)$ the bioconvection Rayleigh number, $\mathrm{Nb}\left(=\frac{\tau D_B(C_w-C_\infty)}{\Delta C \nu_f}\right)$ the Brownian motion variable, $\beta_1\left(=\frac{h_f}{k_f\sqrt{\frac{a}{\nu_f}}}\right)$ the thermal Biot number, $\mathrm{Pr}\left(=\frac{\nu_f}{\alpha_f}\right)$ the Prandtl number, $\mathrm{Sc}\left(=\frac{\nu_f}{D_B}\right)$ the Schmidt number, $\mathrm{Rd}\left(=\frac{16\sigma^* {T_\infty}^3}{3k^* k_f}\right)$ the radiation variable, $\beta_2\left(=\frac{h_w}{D_B\sqrt{\frac{a}{\nu_f}}}\right)$ the solutal

Biot number, $Q\left(=\frac{Q_0}{a(\rho c_p)}\right)$ the heat generation parameter, $\mathrm{Nt}\left(=\frac{\tau D_\mathrm{T}(T_\mathrm{w}-T_\infty)}{T_\infty \nu_\mathrm{f}}\right)$ the thermophoresis variable, $\beta_3\left(=\frac{h_\mathrm{n}}{D_\mathrm{n}\sqrt{\frac{a}{\nu_\mathrm{f}}}}\right)$ the microorganism Biot number, $\mathrm{Lb}\left(=\frac{\nu_\mathrm{f}}{D_\mathrm{m}}\right)$ the bioconvective Lewis number, $\gamma\left(=\frac{k_\mathrm{r}}{a}\right)$ the reaction variable, $\Omega\left(=\frac{N_\infty}{(N_\mathrm{w}-N_\infty)}\right)$ the microorganisms concentration difference factor and $\mathrm{Pe}\left(=\frac{bW_\mathrm{c}}{D_\mathrm{m}}\right)$ the Peclet number.

3 Entropy generation

In mathematical form one can express that:[39–45]

$$N_\mathrm{G}=\frac{k_\mathrm{f}}{{T_\infty}^2}\left(1+\frac{16\sigma^* {T_\infty}^3}{3k^* k_\mathrm{f}}\right)\left(\frac{\partial T}{\partial y}\right)^2+\frac{\sigma_f {B_0}^2}{T_\infty}u^2+\frac{RD_\mathrm{B}}{T_\infty}\left(\frac{\partial T}{\partial y}\frac{\partial C}{\partial y}\right)+\frac{RD_\mathrm{B}}{C_\infty}\left(\frac{\partial C}{\partial y}\right)^2. \tag{13}$$

Non-dimensional form is

$$S_\mathrm{G}=\alpha_1(1+\mathrm{Rd})\theta'^2+M\mathrm{Br}\xi^2 f'^2+L\theta'\phi'+L\frac{\alpha_2}{\alpha_1}\phi'^2, \tag{14}$$

in which R indicates the real gas constant, $S_\mathrm{G}\left(=\frac{N_\mathrm{G}\nu_\mathrm{f}T_\infty}{k_\mathrm{f}a(T_\mathrm{w}-T_\infty)}\right)$ the entropy rate, $\alpha_1\left(=\frac{(T_\mathrm{w}-T_\infty)}{T_\infty}\right)$ the temperature difference variable, $\mathrm{Br}\left(=\frac{\mu_\mathrm{f}(al)^2}{k_\mathrm{f}(T_\mathrm{w}-T_\infty)}\right)$ the Brinkman number, $\alpha_2\left(=\frac{(C_\mathrm{w}-C_\infty)}{C_\infty}\right)$ the concentration difference variable and $L\left(=\frac{RD_\mathrm{B}(C_\mathrm{w}-C_\infty)}{k_\mathrm{f}}\right)$ the diffusion variable.

4 Solution methodology

We consider $\frac{\partial(\cdot)}{\partial\xi}=0$ and denoting $\frac{\partial(\cdot)}{\partial\eta}$ by prime in eqn (8)–(12). We can express that

$$f'''+ff''-f'^2+2K\left(f''^2+f'f'''\right)-Mf'+\frac{\lambda}{\xi}(\theta-\beta_1^*\phi-\beta_2^*\chi)=0, \tag{15}$$

$$(1+\mathrm{Rd})\theta''+\mathrm{Pr}f\theta'+M\mathrm{Pr}Ec\xi^2 f'^2+\mathrm{PrNb}\theta'\phi'+\mathrm{PrNt}\theta'^2+\mathrm{Pr}Q\theta=0, \tag{16}$$

$$\phi''+\mathrm{Sc}f\phi'+\frac{\mathrm{Nt}}{\mathrm{Nb}}\theta''-\mathrm{Sc}\gamma\phi=0, \tag{17}$$

$$\chi''+\mathrm{Lb}f\chi'-\mathrm{Pe}\left(\Omega\phi''+\chi\phi''+\chi'\phi'\right)=0, \tag{18}$$

$$\left.\begin{array}{c} f'(0)=1,\ f(0)=0,\ \theta'(0)=-\beta_1(1-\theta(0)),\\ \phi'(0)=-\beta_2(1-\phi(0)),\ \chi'(0)=-\beta_3(1-\chi(0))\\ f'(\infty)=0,\ \theta(\infty)=0,\ \phi(\infty)=0,\ \chi(\infty)=0 \end{array}\right\}. \tag{19}$$

4.1 Numerical scheme

The ND-solve technique computes the analysis. The Mathematica software is employed to get the numerical solution. For this we set

$$\left.\begin{array}{c} f=y_1^*,\ f'=y_2^*,\ f''=y_3^*,\ f'''={y'}_3^*\\ \theta=y_4^*,\ \theta'=y_5^*,\ \theta''={y'}_5^*\\ \phi=y_6^*,\ \phi'=y_7^*,\ \phi''={y'}_7^*\\ \chi=y_8^*,\ \chi'=y_9^*,\ \chi''={y'}_9^* \end{array}\right\}, \tag{20}$$

$$\left.\begin{array}{c} {y'}_3^*=y_2^*-y_1^*y_2^*-2K\left({y_3}^{*2}-y_2^*{y'}_3^*\right)-My_2^*\\ -\frac{\lambda}{\xi}\left(y_4^*-\beta_1^*y_6^*-\beta_2^*y_8^*\right) \end{array}\right\}, \tag{21}$$

$${y'}_5^*=\frac{-\mathrm{Pr}}{(1+\mathrm{Rd})}\left[y_1^*y_5^*+MEc\xi^2{y_2}^{*2}+\mathrm{Nb}y_5^*y_5^*+\mathrm{Nt}{y_5}^{*2}+Qy_4^*\right], \tag{22}$$

$${y'}_7^*=-\mathrm{Sc}y_1^*y_7^*-\frac{\mathrm{Nt}}{\mathrm{Nb}}{y'}_5^*+\mathrm{Sc}\gamma y_6^*, \tag{23}$$

$${y'}_9^*=-\mathrm{Lb}y_1^*y_9^*-\mathrm{Pe}\left(\Omega{y'}_7^*+y_8^*{y'}_7^*+y_7^*y_9^*\right) \tag{24}$$

with

$$\left.\begin{array}{c} y_1^*(0)=0,\ y_2^*(0)=1,\ y_5^*(0)=-\beta_1\left(1-y_4^*(0)\right)\\ y_7^*(0)=-\beta_2\left(1-y_6^*(0)\right),\ y_9^*(0)=-\beta_3\left(1-y_8^*(0)\right)\\ y_2^*(\infty)=0,\ y_4^*(\infty)=0,\ y_6^*(\infty)=0,\ y_8^*(\infty)=0 \end{array}\right\}. \tag{25}$$

5 Results validation

A comparative study of the present investigation with Kaswan *et al.*[46] is constructed in Table 1 in a limiting sense. From Table

Table 1 Thermal transport rate comparison with Kaswan *et al.*[46]

Pr	Kaswan *et al.*[46]	Present results
0.07	0.065539	0.065536
0.7	0.164035	0.164039
1.0	0.418237	0.418235
2.0	0.826737	0.826738
7.0	1.804291	1.804295
20.0	3.256791	3.256797
70.0	6.346675	6.346679

1 it is clearly detected that results here are in excellent agreement.

6 Graphical analysis

In this section, the physical description of emerging variables is organized.

6.1 Velocity

Fig. 2 displays the behavior of the magnetic variable for velocity. Physically the magnetic field enhances the Lorentz force which induces a resistance in the liquid flow region and the velocity declines. Fig. 3 shows the impact of the material variable on $(f'(\eta))$. Increasing values of the material variable lead to viscous force reduction which intensifies the velocity. Fig. 4 displays the outcomes of the buoyancy ratio variable for velocity. Here reduction in velocity occurs for the buoyancy ratio variable. Fig. 5 elucidates the impact of the bioconvection Rayleigh number. A larger approximation of the bioconvection Rayleigh number (β_2^*) corresponds to a decline in liquid flow $(f'(\eta))$.

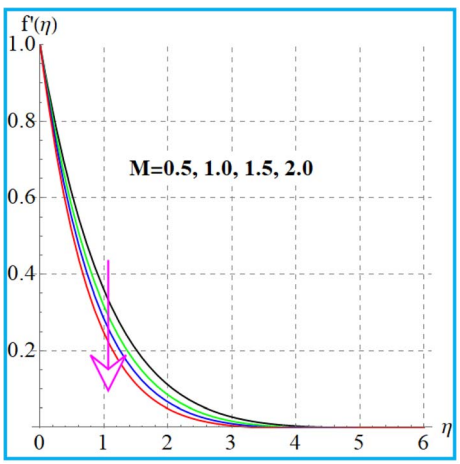

Fig. 2 $f'(\eta)$ variation *versus* M.

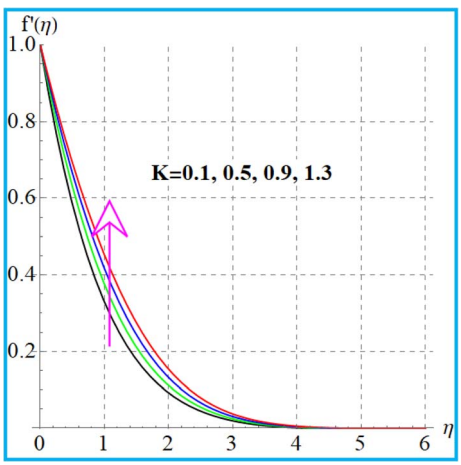

Fig. 3 $f'(\eta)$ variation *versus* K.

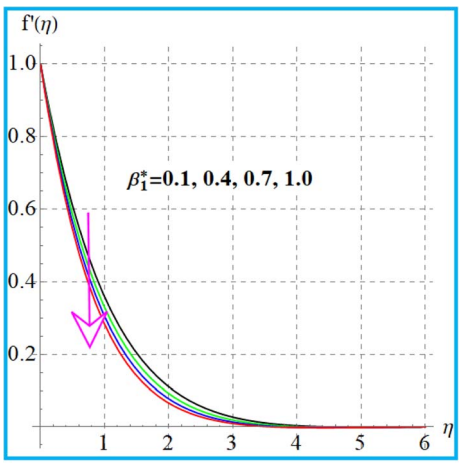

Fig. 4 $f'(\eta)$ variation *versus* β_1^*.

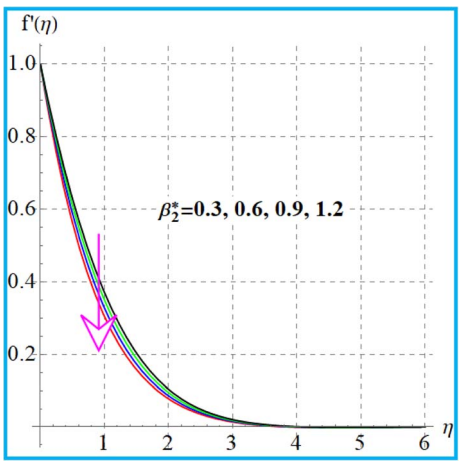

Fig. 5 $f'(\eta)$ variation *versus* β_2^*.

6.2 Temperature

The feature of temperature distribution for the magnetic field is illustrated in Fig. 6. A higher magnetic field increases the

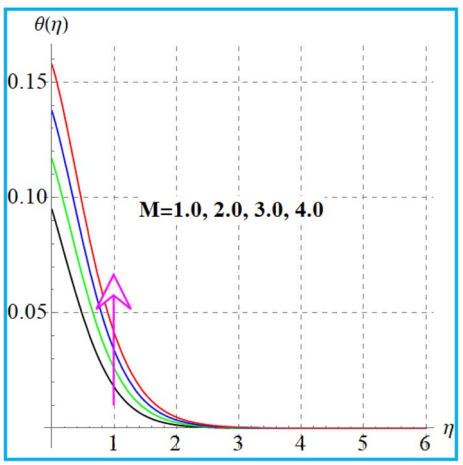

Fig. 6 $\theta(\eta)$ variation *versus* M.

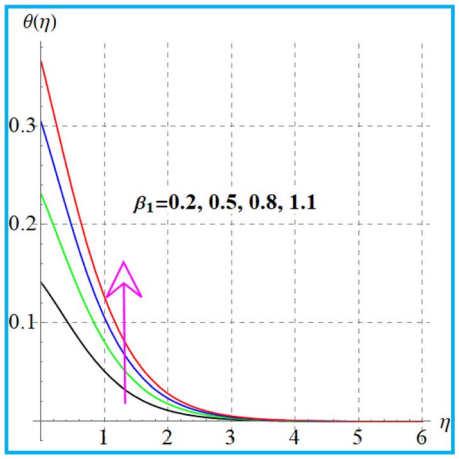

Fig. 7 $\theta(\eta)$ *versus* β_1.

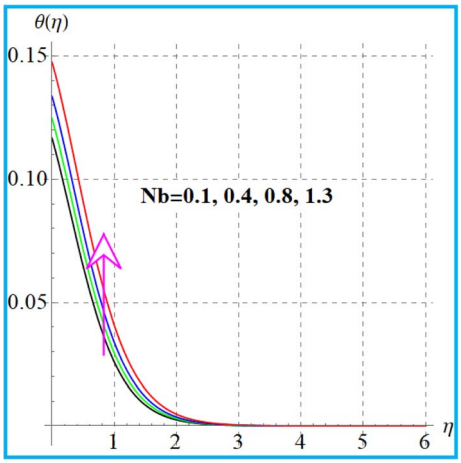

Fig. 10 $\theta(\eta)$ *versus* Nb.

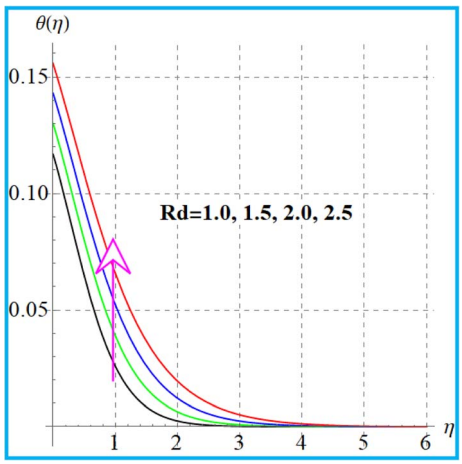

Fig. 8 $\theta(\eta)$ *versus* Rd.

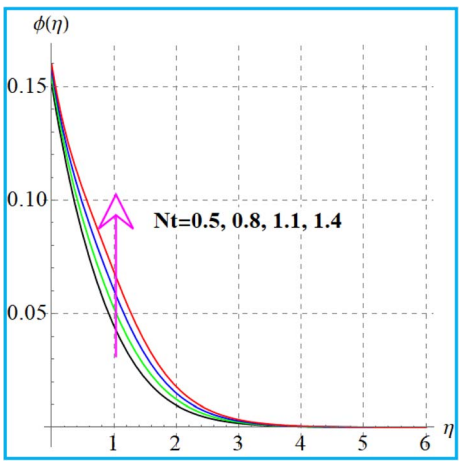

Fig. 11 $\phi(\eta)$ *versus* Nt.

Lorentz force which produces disturbance in the flow region and consequently the kinetic energy of the system is increased. Therefore thermal distribution is intensified. Fig. 7 shows the outcomes of (β_1) on temperature. An enhancement in thermal distribution occurs for a higher thermal Biot number. Results of radiation for temperature are portrayed in Fig. 8. As anticipated,

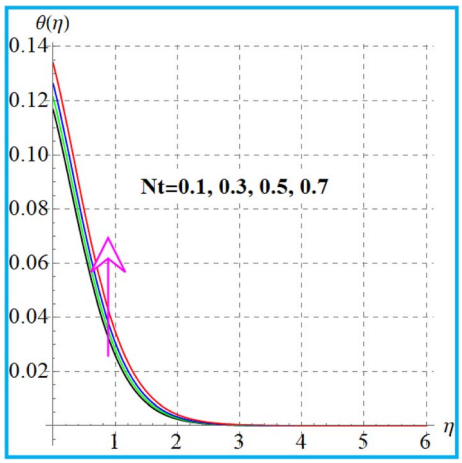

Fig. 9 $\theta(\eta)$ *versus* Nt.

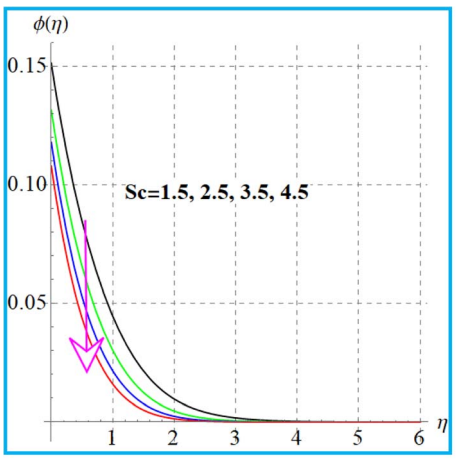

Fig. 12 $\phi(\eta)$ *versus* Sc.

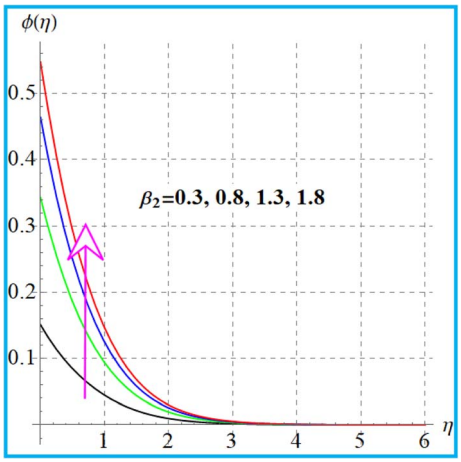

Fig. 13 $\phi(\eta)$ *versus* β_2.

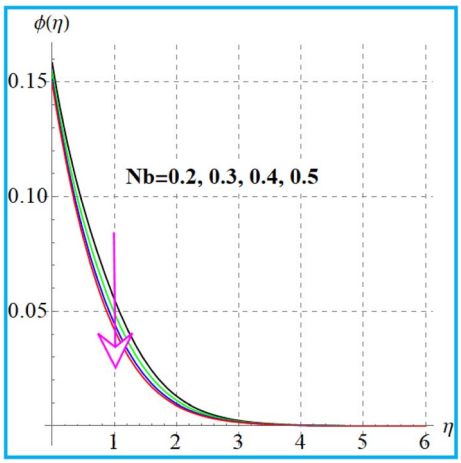

Fig. 14 $\phi(\eta)$ *versus* Nb.

higher radiation impact intensified the thermal field. Fig. 9 and 10 display (Nt) and (Nb) variations for temperature. A larger approximation of (Nt) corresponds to augmentation of the temperature. Additionally, it is seen through Fig. 10 that temperature improves with a higher random motion (Nb) variable.

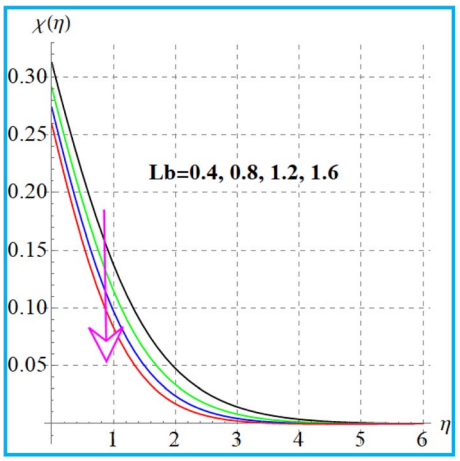

Fig. 15 $\chi(\eta)$ *versus* Lb.

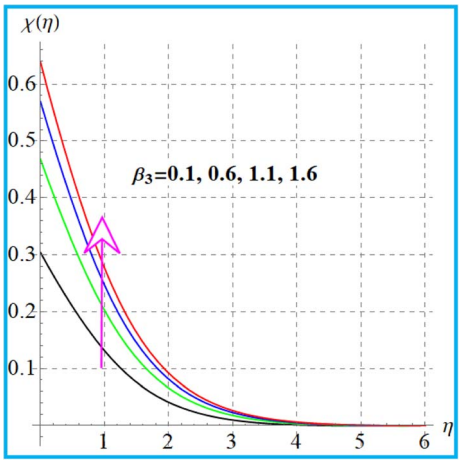

Fig. 16 $\chi(\eta)$ *versus* β_3.

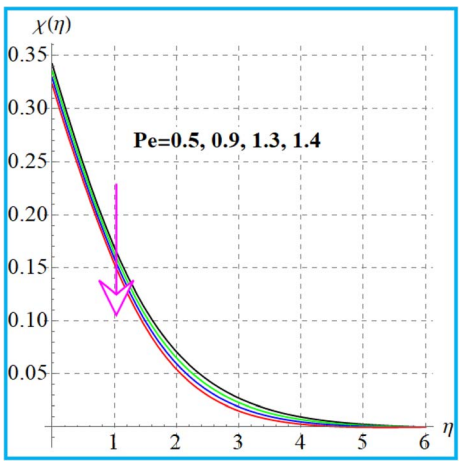

Fig. 17 $\chi(\eta)$ *versus* Pe.

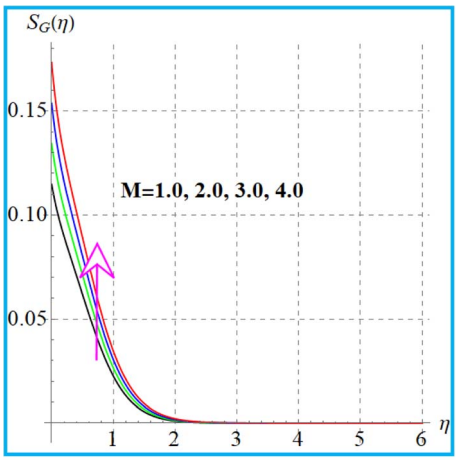

Fig. 18 $S_G(\eta)$ *versus* M.

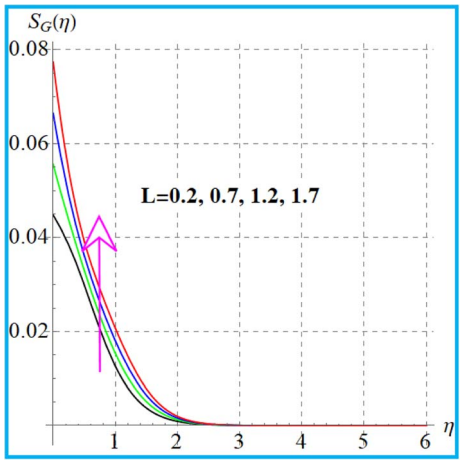

Fig. 19 $S_G(\eta)$ *versus* L.

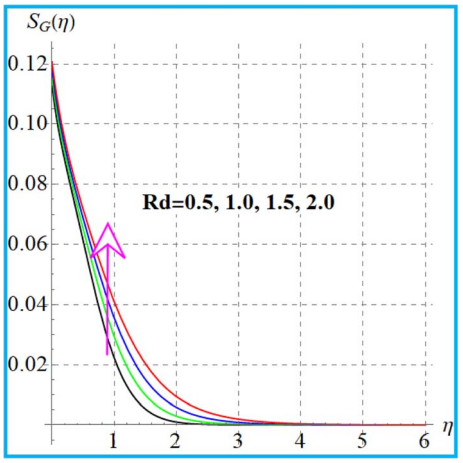

Fig. 21 $S_G(\eta)$ *versus* Rd.

6.3 Concentration

Fig. 11 illustrates the impact of (Nt) on concentration. An increment in concentration occurs through a higher thermophoresis variable. The feature of concentration $(\phi(\eta))$ for (Sc) is depicted in Fig. 12. Here due to an increase in (Sc), the concentration decays due to reduction in mass diffusivity. Fig. 13 displays the variation of (β_2) for concentration. Clearly, the concentration boosts up for a higher solutal Biot number. Additionally, it is evident through Fig. 14 that concentration decays with a random motion variable.

6.4 Microorganism field

Fig. 15 exhibits the result of the bioconvection Lewis number on $(\chi(\eta))$. Clearly, microorganism field degradation is detected against a higher bioconvection Lewis number (Lb). The influence of (β_3) on the microorganism field $(\chi(\eta))$ is shown in Fig. 16. A higher estimation of (β_3) leads to augmentation of the microorganism $(\chi(\eta))$ field. The graphical feature of $(\chi(\eta))$ *versus* the Peclet number is portrayed in Fig. 17. A clearly decreasing trend of microorganisms $(\chi(\eta))$ is witnessed for a higher Peclet (Pe) number.

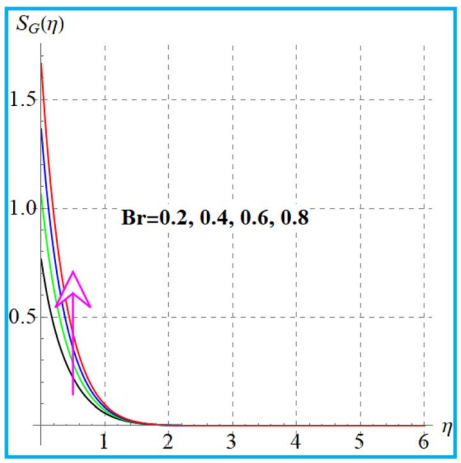

Fig. 20 $S_G(\eta)$ *versus* Br.

6.5 Entropy production

Fig. 18 shows the entropy variation against the magnetic variable. With an increase in the magnetic field the Lorentz force causes more resistance in the flow region. As a result, the internal energy of the system increases and consequently the entropy rate is augmented. Fig. 19 displays the impact of the diffusion parameter (L) on $(S_G(\eta))$. Here entropy rises against the diffusion variable. Effects of (Br) on the entropy rate are given in Fig. 20. An increment in entropy generation is found for a larger Brinkman number due to a larger kinetic energy. Fig. 21 elucidates the outcomes of the radiation parameter (Rd) for $(S_G(\eta))$. The entropy rate against radiation is enhanced.

7 Closing remarks

Here the magnetized bioconvective flow of the Reiner–Rivlin nanomaterial by convective conditions is examined. Entropy analysis in the presence of chemical reaction is addressed. Gyrotactic micro-organisms are taken into account. Key points of recent analysis are given below.

- Reduction occurs in liquid flow for the magnetic field and bioconvection Rayleigh number.
- Velocity improves for higher values of the material variable while the reverse impact holds for the buoyancy ratio variable.
- Temperature enhancement is noted for thermophoresis and radiation variables.
- An increase in temperature distribution and entropy rate is witnessed for the magnetic field.
- Higher random motion leads to temperature enhancement.
- A larger approximation of the thermal Biot number intensifies the temperature distribution.
- The reverse trend holds for concentration against random motion and thermophoresis variables.

• A decline in concentration occurs for a higher Schmidt number.

• Concentration increases for a higher solutal Biot number.

• Reduction in microorganisms occurs *versus* the Peclet number.

• Microorganism field decays against a higher bioconvection Lewis number.

• Entropy rate has similar behavior against radiation and diffusion variables.

• Entropy rate increases *versus* a larger Brinkman number.

Conflicts of interest

There are no conflicts to declare.

References

1 S. U. S. Choi, Enhancing thermal conductivity of fluids with nanoparticles, *J. Fluids Eng.*, 1995, **231**, 99–106.

2 J. A. Eastman, S. U. S. Choi, S. Li, W. Yu and L. J. Thompson, Anomalously increased effective thermal conductivities of ethylene glycol-based nanofluids containing copper nanoparticles, *Appl. Phys. Lett.*, 2001, **78**, 718–720.

3 J. Buongiorno, Convective transport in nanofluids, *J. Heat Transf.*, 2006, **128**, 240–250.

4 A. Shahzad, M. Imran, M. Tahir, S. A. Khan, A. Akgül, S. Abdullaev, C. Park, H. Y. Zahran and I. S. Yahia, Brownian motion and thermophoretic diffusion impact on Darcy-Forchheimer flow of bioconvective micropolar nanofluid between double disks with Cattaneo-Christov heat flux, *Alexandria Eng. J.*, 2023, **62**, 1–15.

5 M. Waqas, M. I. Khan, T. Hayat, M. M. Gulzar and A. Alsaedi, Transportation of radiative energy in viscoelastic nanofluid considering buoyancy forces and convective conditions, *Chaos, Solitons Fractals*, 2020, **130**, DOI: 10.1016/j.chaos.2019.109415.

6 N. Anjum, W. A. Khan, A. Hobiny, M. Azam, M. Waqas and M. Irfan, Numerical analysis for thermal performance of modified Eyring Powell nanofluid flow subject to activation energy and bioconvection dynamic, *Chaos, Solitons Fractals*, 2022, **39**, DOI: 10.1016/j.csite.2022.102427.

7 F. Mabood, M. D. Shamshuddin and S. R. Mishra, Characteristics of thermophoresis and Brownian motion on radiative reactive micropolar fluid flow towards continuously moving flat plate: HAM solution, *Math. Comput. Simul.*, 2022, **191**, 187–202.

8 G. Kalpana, K. R. Madhura and R. B. Kudenatti, Numerical study on the combined effects of Brownian motion and thermophoresis on an unsteady magnetohydrodynamics nanofluid boundary layer flow, *Math. Comput. Simul.*, 2022, **200**, 78–96.

9 A. Riaz, T. Abbas, A. Zeeshan and M. H. Doranehgard, Entropy generation and MHD analysis of a nanofluid with peristaltic three dimensional cylindrical enclosures, *Int. J. Numer. Methods Heat Fluid Flow*, 2021, **31**, 2698–2714.

10 M. Hussain and M. Sheremet, Convection analysis of the radiative nanofluid flow through porous media over a stretching surface with inclined magnetic field, *Int. Commun. Heat Mass Transfer*, 2023, **140**, DOI: 10.1016/j.icheatmasstransfer.2022.106559.

11 W. A. Khan, M. Waqas, S. Kadry, Z. Asghar, S. Z. Abbas and M. Irfan, On the evaluation of stratification based entropy optimized hydromagnetic flow featuring dissipation aspect and Robin conditions, *Comput. Methods Programs Biomed.*, 2020, **190**, DOI: 10.1016/j.cmpb.2020.105347.

12 M. Jawad, M. K. Hameed, K. S. Nisar and A. H. Majeed, Darcy-Forchheimer flow of Maxwell nanofluid flow over a porous stretching sheet with Arrhenius activation energy and nield boundary conditions, *Chaos, Solitons Fractals*, 2023, **44**, DOI: 10.1016/j.csite.2023.102830.

13 F. Shah, T. Hayat and S. Momani, Non-similar analysis of the Cattaneo-Christov model in MHD second-grade nanofluid flow with Soret and Dufour effects, *Alexandria Eng. J.*, 2023, **70**, 25–35.

14 N. Vijay and K. Sharma, Dynamics of stagnation point flow of Maxwell nanofluid with combined heat and mass transfer effects: A numerical investigation, *Int. Commun. Heat Mass Transfer*, 2023, **141**, DOI: 10.1016/j.icheatmasstransfer.2022.106545.

15 C. Sulochana, G. P. Ashwinkumar and N. Sandeep, Transpiration effect on stagnation point flow of a Carreau nanofluid in the presence of thermophoresis and Brownian motion, *Alexandria Eng. J.*, 2016, **55**, 1151–1157.

16 I. Waini, K. B. Hamzah, N. S. Khashi'ie, N. A. Zainal, A. R. M. Kasim, A. Ishak and I. Pop, Brownian and thermophoresis diffusion effects on magnetohydrodynamic Reiner-Philippoff nanofluid flow past a shrinking sheet, *Alexandria Eng. J.*, 2023, **67**, 183–192.

17 A. Alsaedi, A. Razaq, T. Hayat and S. A. Khan, Modeling and simulation of Cattaneo-Christov fluxes in entropy induced flow through Reiner–Rivlin fluid conveying tiny particles, *Alexandria Eng. J.*, 2023, **74**, 1–19.

18 T. J. Pedley, N. A. Hill and J. O. Kessler, The growth of bioconvection patterns in a uniform suspension of gyrotactic micro-organisms, *J. Fluid Mech.*, 1988, **195**, 223–237.

19 T. J. Pedley and J. O. Kessler, A new continuum model for suspensions of gyrotactic micro-organisms, *J. Fluid Mech.*, 1990, **212**, 155–182.

20 B. Kada, I. Hussain, A. A. Pasha, W. A. Khan, M. Tabrez, K. A. Juhany, M. Bourchak and R. Othman, Significance of gyrotactic microorganism and bioconvection analysis for radiative Williamson fluid flow with ferromagnetic nanoparticles Therm, *Sci. Eng. Prog.*, 2023, **39**, DOI: 10.1016/j.tsep.2023.101732.

21 A. Majeed, A. Zeeshan, N. Amin, N. Ijaz and T. Saeed, Thermal analysis of radiative bioconvection magnetohydrodynamic flow comprising gyrotactic microorganism with activation energy, *J. Therm. Anal. Calorim.*, 2021, **143**, 2545–2556.

22 M. Waqas, W. A. Khan, A. A. Pasha, N. Islam and M. M. Rahman, Dynamics of bioconvective Casson nanoliquid from a moving surface capturing gyrotactic microorganisms, magnetohydrodynamics and

stratifications, *Therm. Sci. Eng. Prog.*, 2022, **36**, DOI: 10.1016/j.tsep.2022.101492.

23 M. Azam, T. Xu, F. Mabood and M. Khan, Non-linear radiative bioconvection flow of cross nano-material with gyrotactic microorganisms and activation energy, *Int. Commun. Heat Mass Transfer*, 2021, **127**, DOI: 10.1016/j.icheatmasstransfer.2021.105530.

24 N. Fatima, W. Belhadj, K. S. Nisar, Usman, M. K. Alaoui, M. B. Arain and N. Ijaz, Heat and mass transmission in a boundary layer flow due to swimming of motile gyrotactic microorganisms with variable wall temperature over a flat plate, *Chaos, Solitons Fractals*, 2023, **45**, DOI: 10.1016/j.csite.2023.102953.

25 A. K. Kushwaha and Y. D. Sharma, Significance of vertical vibration on the stability of thermo-bioconvection in a suspension of oxytactic microorganisms, *Int. Commun. Heat Mass Transfer*, 2022, **133**, DOI: 10.1016/j.icheatmasstransfer.2022.105943.

26 A. A. Avramenko, Y. Y. Kovetska and I. V. Shevchuk, Lorentz approach for analysis of bioconvection instability of gyrotactic motile microorganisms, *Chaos, Solitons Fractals*, 2023, **166**, DOI: 10.1016/j.chaos.2022.112957.

27 N. Biswas, D. K. Mandal, N. K. Manna and A. C. Benim, Enhanced energy and mass transport dynamics in a thermo-magneto-bioconvective porous system containing oxytactic bacteria and nanoparticles: Cleaner energy application, *Energy*, 2023, **263**, DOI: 10.1016/j.energy.2022.125775.

28 A. Majeed, N. Golsanami, B. Gong, Q. A. Ahmad, S. Rifaqat, A. Zeeshan and F. M. Noori, Analysis of thermal radiation in magneto-hydrodynamic motile gyrotactic micro-organisms flow comprising tiny nanoparticle towards a nonlinear surface with velocity slip, *Alexandria Eng. J.*, 2023, **66**, 543–553.

29 A. S. M. Aljaloud, L. Manai and I. Tlili, Bioconvection flow of Cross nanofluid due to cylinder with activation energy and second order slip features, *Chaos, Solitons Fractals*, 2023, **42**, DOI: 10.1016/j.csite.2023.102767.

30 R. R. Kairi, S. Roy and S. Raut, Stratified thermosolutal Marangoni bioconvective flow of gyrotactic microorganisms in Williamson nanofluid, *Eur. J. Mech. B/Fluids*, 2023, **97**, 40–52.

31 S. Hussain, A. M. Aly and N. Alsedias, Bioconvection of oxytactic microorganisms with nano-encapsulated phase change materials in an omega-shaped porous enclosure, *J. Energy Storage*, 2022, **56**, DOI: 10.1016/j.est.2022.105872.

32 M. Irfan, W. A. Khan, A. A. Pasha, M. I. Alam, N. Islam and M. Zubair, Significance of non-Fourier heat flux on ferromagnetic Powell-Eyring fluid subject to cubic autocatalysis kind of chemical reaction, *Int. Commun. Heat Mass Transfer*, 2022, **138**, DOI: 10.1016/j.icheatmasstransfer.2022.106374.

33 S. A. Khan, T. Hayat and A. Alsaedi, Entropy generation in chemically reactive flow of Reiner–Rivlin liquid conveying tiny particles considering thermal radiation, *Alexandria Eng. J.*, 2023, **66**, 257–268.

34 M. Reiner, A mathematical theory of dilatancy, *Am. J. Math.*, 1945, **67**, 350–362.

35 R. S. Rivlin, The hydrodynamics of non-Newtonian fluids, *Proc. R. Soc. A: Math. Phys. Eng. Sci.*, 1948, **193**, 260–281.

36 M. Tabassum and M. Mustafa, A numerical treatment for partial slip flow and heat transfer of non-Newtonian Reiner–Rivlin fluid due to rotating disk, *Int. J. Heat Mass Transfer*, 2018, **123**, 979–987.

37 B. Sahoo, R. A. V. Gorder and H. I. Andersson, Steady revolving flow and heat transfer of a non-Newtonian Reiner–Rivlin fluid, *Int. Commun. Heat Mass Transfer*, 2012, **39**, 336–342.

38 S. A. Khan, T. Hayat and A. Alsaedi, Simultaneous features of Soret and Dufour in entropy optimized flow of Reiner–Rivlin fluid considering thermal radiation, *Int. Commun. Heat Mass Transfer*, 2022, **137**, DOI: 10.1016/j.icheatmasstransfer.2022.106297.

39 M. A. Sadiq and T. Hayat, Entropy optimized flow of Reiner–Rivlin nanofluid with chemical reaction subject to stretchable rotating disk, *Alexandria Eng. J.*, 2022, **61**, 3501–3510.

40 Z. Abbas, M. Naveed, M. Hussain and N. Salamat, Analysis of entropy generation for MHD flow of viscous fluid embedded in a vertical porous channel with thermal radiation, *Alexandria Eng. J.*, 2020, **59**, 3395–3405.

41 Y. Liu, J. Xing and Y. Jian, Heat transfer and entropy generation analysis of electroosmotic flows in curved rectangular nanochannels considering the influence of steric effects, *Int. Commun. Heat Mass Transfer*, 2022, **139**, DOI: 10.1016/j.icheatmasstransfer.2022.106501.

42 R. Sarma, A. K. Shukla, H. S. Gaikwad, P. K. Mondal and S. Wongwises, Effect of conjugate heat transfer on the thermo-electro-hydrodynamics of nanofluids: entropy optimization analysis, *J. Therm. Anal. Calorim.*, 2022, **147**, 599–614.

43 B. Iftikhar, T. Javed and M. A. Siddiqu, Entropy generation analysis during MHD mixed convection flow of non-Newtonian fluid saturated inside the square cavity, *J. Comput. Sci.*, 2023, **66**, DOI: 10.1016/j.jocs.2022.101907.

44 W. Ibrahim and D. Gamachu, Entropy generation in radiative magnetohydrodynamic mixed convective flow of viscoelastic hybrid nanofluid over a spinning disk, *Heliyon*, 2022, **8**, DOI: 10.1016/j.heliyon.2022.e1185.

45 A. Alsaedi, A. Razaq, T. Hayat and S. A. Khan, On bioconvective chemically reactive flow involving applications of magnetohydrodynamic and radiation, *Alexandria Eng. J.*, 2023, **75**, 549–563.

46 P. Kaswan, M. Kumar and M. Kumari, Analysis of a bioconvection flow of magnetocross nanofluid containing gyrotactic microorganisms with activation energy using an artificial neural network scheme, *Results Eng.*, 2023, **17**, DOI: 10.1016/j.rineng.2023.101015.